THE INFLUENCE OF MECHANICAL TEST PARAMETERS ON THE OUTCOME OF THE END NOTCH FLEXURE TEST FOR MODE II FRACTURE TOUGHNESS

Ives De Baere, Stefan Jacques and Wim Van Paepegem

[1]Department of Materials Science and Engineering, Ghent University
Technologiepark-Zwijnaarde 903, 9052 Zwijnaarde, Belgium
Email: Ives.DeBaere@UGent.be web page: http://www.composites.ugent.be

Keywords: Fracture toughness, Mode II, End notch Flexure, mechanical testing, carbon fabric, thermoplastic

ABSTRACT

When determining Mode II crack growth behaviour of composite materials, the end notch flexure test is quite commonly used. Using the compliance based beam method, it is a very easy and straightforward test for the determination of the mode II crack fracture toughness, without the need of continuously monitoring the crack length. Sometimes, the problem arises where there is unstable crack growth, but usually this can be solved by performing tests under displacement control and fulfilling a certain geometric demand. However, the influence of certain mechanical test parameters is not yet fully quantified. This study investigates the influence of a number of experimental parameters, such as the difference in thickness of the substrates of the specimen, the positioning of the supporting and loading rods, the influence of friction, both between the substrates and between the specimen and the supports. In order to avoid additional experimental scatter, the influence of these parameters is assessed by finite element analysis using the cohesive model approach. The results will be compared to an analytical solution obtained by linear elastic fracture mechanics as well as to a carbon fibre 5-harness satin weave reinforced polyphenylene sulphide composite.

1 INTRODUCTION

Delamination is one of the most difficult and common types of damage in laminated composite structures due to the relatively weak interlaminar strengths. Delamination starts generally at geometrical discontinuities, such as laminate free edges and cut-outs. This is so because the state of stress close to a free edge in a laminate is three-dimensional, with nonzero interlaminar stresses, which grow without bound due to a singularity in the stress field at the intersection of the free-edge and the interface. Delaminations may arise under various circumstances, e.g. when subjected to transverse concentrated loads, such as low/high velocity impacts arising from a falling mass, and propagate due to the loads of the structure such as dynamic loading. Finally the behaviour of the entire structure changes and in most cases a failure is unavoidable.

For this manuscript, the emphasis lies on mode II delamination growth and the experimental setup of choice is the End Notch Flexure test. The objective of an End Notch Flexural (ENF) test is to determine the G_{IIc} for an interlaminar interface. In the research community, a lot of research has been made on the determination of the mode II critical strain energy release G_{IIc} with the following three most popular experimental configurations: (i) the End Notch Flexure (ENF) test [1], (ii) the End Loaded Split (ELS) test [2, 3] and (iii) the 4ENF test [4] . The ENF test is a simple three point bending test on a pre-cracked test specimen (Figure 1). A disadvantage of the ENF test method is the possibility of having unstable crack propagation. Referring to the work of Carlsson and Gillespie (1989) [3, 4], the ENF test requires a ratio $a/L > 0.7$ to avoid this.
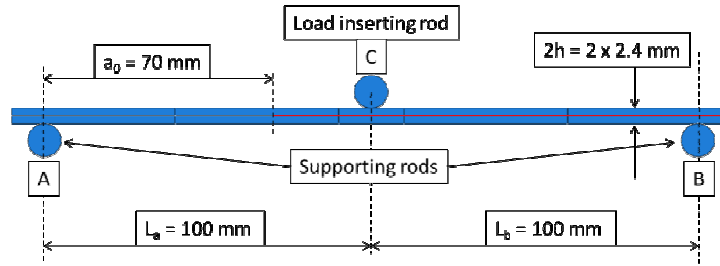
Figure 1 Geometrical properties of the ENF model

The goal of this research is to study the influence of a number of experimental test parameters on the outcome of the ENF test, such as the difference in thickness of the substrates of the specimen, the positioning of the supporting and loading rods, the influence of friction, both between the substrates and between the specimen and the supports. However, most of these parameters are in fact very difficult to control/influence in real life, e.g. how to determine and/or control the friction coefficient within the delaminated area. Moreover, when conducting experiments, there is always an amount of scatter on the results, simply because there is (small) variability within the properties of the composite. Hence, it was chosen to investigate the influence of the mentioned parameters in a numerical way, offering more control over the values and eliminating the natural experimental scatter.

To model the crack growth, the cohesive zone method, using cohesive elements, is considered and the bilinear softening equation (Figure 2) is used.
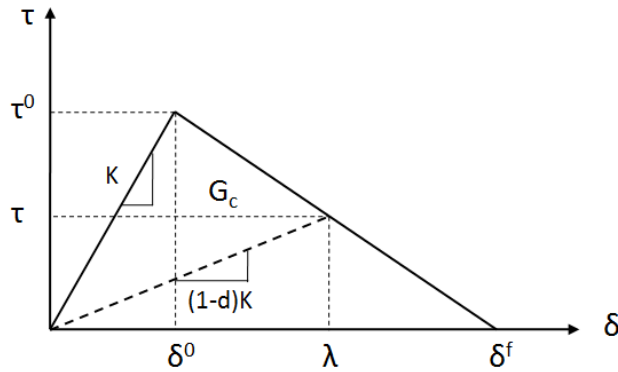

Figure 2 Bilinear cohesive traction separation law [5]

The cohesive zone model with the boundary value problem, the kinematics and constitutive relations for the formulation of the model for the delamination initiation and propagation are nicely presented by Turon and Camanho (2006) in [5].

An important remark must be made. The purpose was to investigate the experimental parameters in a numerical way, to avoid experimental scatter, but off course, it has to be assured that the numerical parameters, which influence the cohesive modelling results, are set to the correct values. Hence, the combination of the different parameters like stiffness, strength, numerical stabilization, output frequency, mesh size are always optimized first, before conclusions with respect to the experimental parameters are drawn. More details on how this optimization can be done, are found in [6].

2   MATERIAL AND METHODS

2.1.   Material

The material considered here is a polyphenylene sulphide (PPS) reinforced with a 5-harness weave carbon fibre (CF) fabric also known as CETEX. The plates with the insertion of a kapton film in the midplane of the $[(0, 90)_4, (90, 0)_4]_s$ stacking exist of a total of 16 layers of fabric. These plates were produced and delivered by TenCate (Netherlands). The plates were sawed using a diamond saw in the

dimensions corresponding to Figure 1 with a width of 25mm. The elastic properties for the CETEX CF/PPS composite can be found in Table 1 .

CF/PPS (CETEX) Elastic properties								
E_{11}, [GPa]	E_{22}, [GPa]	E_{33}, [GPa]	v_{12}, [-]	v_{13}, [-]	v_{23}, [-]	G_{12}, [MPa]	G_{13}, [MPa]	G_{23}, [MPa]
56.2	56.21	10.66	0.08	0.42	0.42	4390.28	3227.19	3228.68

Table 1 : Material properties used for the construction of the DCB model of the CETEX material

The dimensions of the test samples can be found Table 2

Specimen	Width, [mm]	Half span L, [mm]	Crack length a_0, [mm]	Testing speed, [mm/min]
CET 7	16.1	100.0	70	0.5
CET 8	16.1	100.0	70	1

Table 2 : Dimensions of the CETEX test specimens (CET 7 - CET 8)

The procedure for the calculation of the Mode II G_{IIc} propagation ($G_{IIc, prop}$) and its results can be found in [7] leading to an average $G_{IIc, prop}$ = 3400 J/m².

2.2. Analytical solution for the mode II ENF test

The analytical solution for the ENF test can be split in the three stages of the load-displacement curve as defined earlier [8]. The load and displacement can be calculated with following equations:
Linear part:

$$\delta = \frac{P\left(3a_0^3 + 2L^3\right)}{8E_{11}Bh^3} \tag{1}$$

Displacement and load during crack propagation with a < L:

$$\delta = \frac{P\left(3a^3 + 2L^3\right)}{8E_{11}Bh^3} \tag{2}$$

$$P = \sqrt{\frac{16G_{IIc}B^2h^3E_{11}}{9a^2}} \tag{3}$$

Displacement and load during crack propagation with a > L:

$$\delta = \frac{P}{2E_{11}Bh^3}\left[2L^3 - \frac{\left(\frac{16}{3}G_{IIc}E_{11}B^2h^3\right)^{3/2}}{4\sqrt{3}P^3}\right] \tag{4}$$

$$P = \sqrt{\frac{16G_{IIc}B^2h^3E_{11}}{9a^2}} \tag{5}$$

where: G_{IIc} = critical mode II strain energy release rate, *[J/m²]*
B = width of the test sample, *[m]*
h = half of the thickness of the test sample, *[m]*
E_{11} = longitudinal Young's modulus, *[Pa]*
P = applied force, *[N]*
a = the crack length, *[m]*
L = half of the span as given in Figure 1, *[m]*

A comparison between the experimental tests for the CET 7 and CET 8 test specimen and the analytically calculated load and displacement curves using the from CET7 and CET8 experimentally derived minimum and maximum values for G_{IIc}, (3379 J/m² and 3674 J/m² respectively [7]) can be found in Figure 10.

3   NUMERICAL SIMULATION

A lot of research has been accomplished on the simulation of the mode II end notched flexure (ENF) test. Again in many cases not all the different parameters are given in order to reproduce the same simulations using the same models and material parameters. Here, the influence of the following experimental parameters on the outcome of the ENF test is investigated:

1. position of the supporting and loading rod on the sample
2. influence of the thickness of the substrates and the strength
3. influence of the friction (internal and external)

The geometrical dimensions of the ENF test sample CET 7 and CET 8, together with the material properties for the CETEX test samples can be found in paragraph 2.1. The geometrical properties of the numerical ENF model can be found in Figure 1.

In between the different rods (Steel) and the contact surfaces of the substrates (PPS) of the ENF sample, friction was taken into account. Friction was also introduced in between the substrates of the sample itself. While the supporting rods are fixed, a displacement is given to the load inserting rod which will introduce the load into the numerical ENF test sample as it is done in real experimental test setups. In order to be sure to capture the different numerical aspects of the ENF simulation, two models, a 2D and a 3D model have been constructed. After a mesh convergence for the two models and stabilization convergence, further study was made using a 2D model existing of 22000 linear quadrilateral elements (CPS4I) and 1400 linear quadrilateral cohesive elements (l = 0.1mm) and 2366 elements for the rods. The 3D model was built using 18400 linear quadrilateral shell elements (S4) and 400 linear quadrilateral cohesive elements with variation in lengths (l_{min} = 0.2mm and l_{max} = 1mm) reducing the calculation time, plus the elements needed to represent the rods. The mode II average critical energy release rates G_{IIc} (= 3400 J/m²) was determined in section 2 and is used in the simulations. The results were exported at each time increment. A stabilization convergence study concerning the viscous regularization factor for the 3D numerical models of the ENF test was performed. The friction coefficient between the PPS substrates and the steel rods equals 0.25 [9] and is simulated with a master-slave contact interaction with a finer mesh of the slave part compared to the master part. The influence of this friction coefficient has been studied by variation of the friction coefficient will be shown in later section 3.1.3. The shear strength of PPS [10] is around 60MPa, therefore this value will be used together with a value of 30MPa and 90MPa in order to show the influence if the strength parameter. A stiffness of 1e6 and a viscous regularization factor between 1e5 – 1e8 was used in the simulations. The 3D model with a strength τ^0 = 90MPa will be considered as a reference in following studies since this value corresponds the closest to the analytical solution.

3.1.   Parametric study

3.1.1.   Position of the rods

The reference model (TRAN A) has a half span L_a = 100 mm and L_b = 100 mm (Figure 1) and this has been changed in order to check the sensitivity of the results to such variations. A study was performed with an asymmetric support with a half span on one side L_a = 100 mm while keeping the original L_b = 98 mm on the other side (Figure 1) and can be find as model TRAN B in Figure 3. A similar simulation was made but with opposite asymmetry with L_a = 98 mm and L_b = 100 mm (Figure 1), see model TRAN C. The results as given in Figure 3 show that some variations may occur when the positions of the rods are changed. For example when comparing model TRAN A, TRAN B and TRAN C, a small shift of the load-displacement curve can be noticed which represents a stiffening of the response due to the decrease of the leverage. One can also see that if the central rod, inducing the

load on the test sample, is slightly shifted (TRAN D and TRAN E), one can obtain a difference in maximum force between the ideal positioning ($L_a = L_b = 100$ mm) and the shifted ones of approximately 3% for this material and configuration.
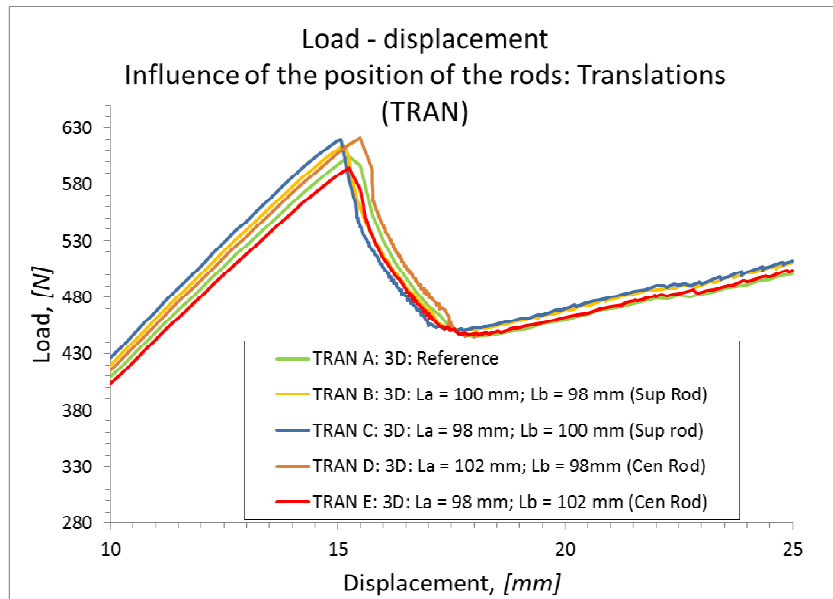

Figure 3 Influence of the position of the rods - Translations - on the numerical load-displacement curves of the ENF simulation

The influence of the rotations of the supporting rods and the central rod as depicted in Figure 4, was investigated. Model ROT B and ROT C show the load-displacement results for the simulations where both supporting rods are rotated like given in point A and point B of Figure 4 by 1 degree respectively 2 degrees. The last model presents the results of a model where only the central, load inserting rod, has been rotated by 2 degrees.
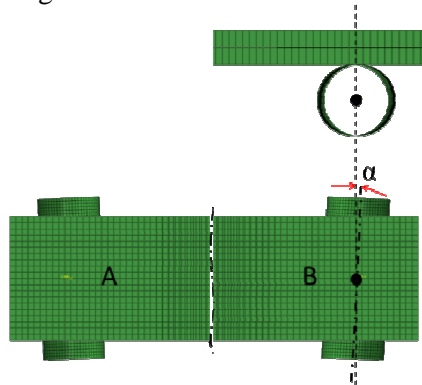

Figure 4 Rotation of a rod by α degrees

A small rotation of the two supporting or the central rods does not have any significant effect on the resulting load-displacement curves, as shown in Figure 5. All the load-displacement curves of the different models coincide with the reference model with the ideally positioned rods.
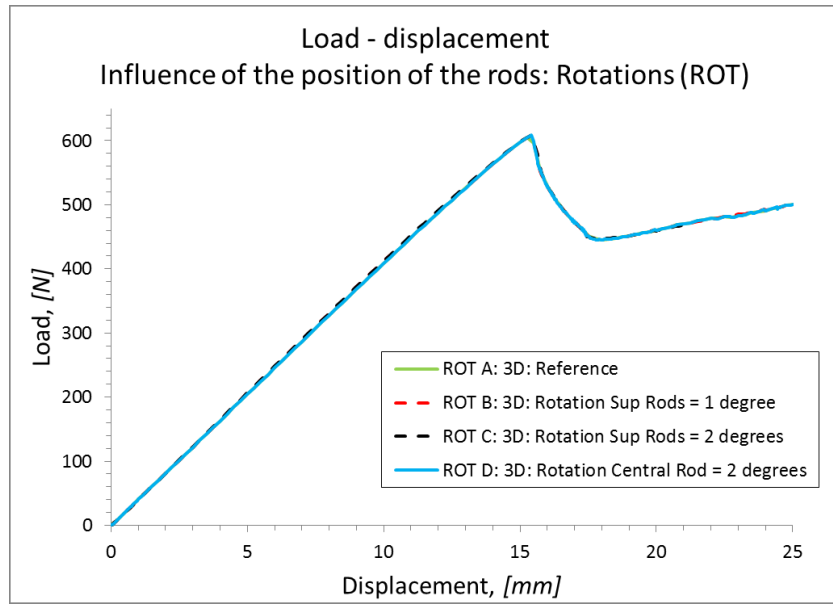
Figure 5 Influence of the position of the rods - Rotations - on the numerical load-displacement curves of the ENF simulation

3.1.2. Influence of the thickness of the substrates and the strength

This study aims to check the influence of the thickness of half of the total thickness of the test sample h (Figure 1). The models used for this study are based on the reference 2D model. The thicknesses of the substrates of this model have been changed from 2 x (h = 2.4 mm) into h_{top} = 2.35 mm and h_{bot} = 2.45 mm. h_{top} represents the thickness of the substrate at the top in contact with the load inserting rod. Additionally, the thickness h_{top} has been reduced to h_{top} = 2.3 mm with h_{bot} = 2.5 mm. The results presented here have been obtained using two strength values, τ_0 = 30 MPa and τ_0 = 90MPa.

The influence of the thickness of the substrates of the ENF simulated test sample cannot be noticed in contrary to the similar graphs shown for the DCB simulation, which can be found in [6]. On the other hand it is clear that the maximum strength τ_0 has a significant impact on the resulting numerical load-displacement curves. Since a decrease in strength, with a constant critical strain energy release rate G_{IIc} and stiffness K, leads to an increase of the final displacement jump at failure δf, it gives a smoother load-displacement curve. The maximum load obtained before failure using a strength τ_0 = 30 MPa is approximately 550N, whereas for τ_0 = 90 MPa the load reaches more than 600 N which is a considerable difference.
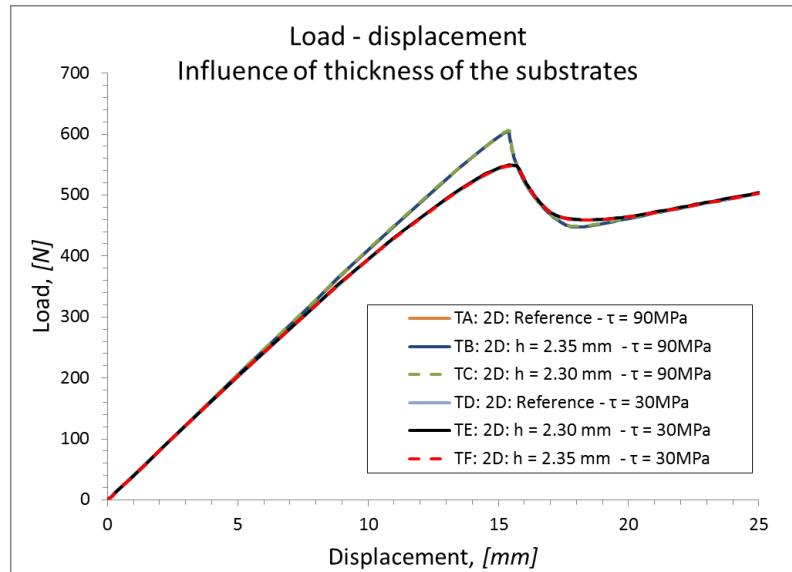
Figure 6 Influence of the thickness of the substrates on the numerical load-displacement curves of the ENF simulation

3.1.3. Influence of Friction

Since it is not always mentioned in the reports or papers dealing with experimental ENF tests what the friction coefficient between the rods and the contact surface of the substrates of the test sample is, a numerical study was effectuated in order to find out what the impact could be on the resulting load-displacement curves. Therefore it was chosen to perform the quasi-static simulations using the 3D reference model with different friction coefficients at multiple failure strengths τ_0 (30, 60 and 90 MPa). Both the impact of the friction between the substrates of the ENF model (INT) as well as the friction at the contact surface between the rods and the substrates (EXT) has been studied. At last a combination of the effect due to the friction at the contact surface and the strength is shown.

Internal friction between the substrates of the model

The influence due to the friction between the surfaces of the substrates of the numerical test sample is very low. Only a small shift of the curve can be noticed comparing a friction coefficient of 0.01 to a friction coefficient of 0.4 leading to a maximum force difference of less than 1%, as can be seen in Figure 7.
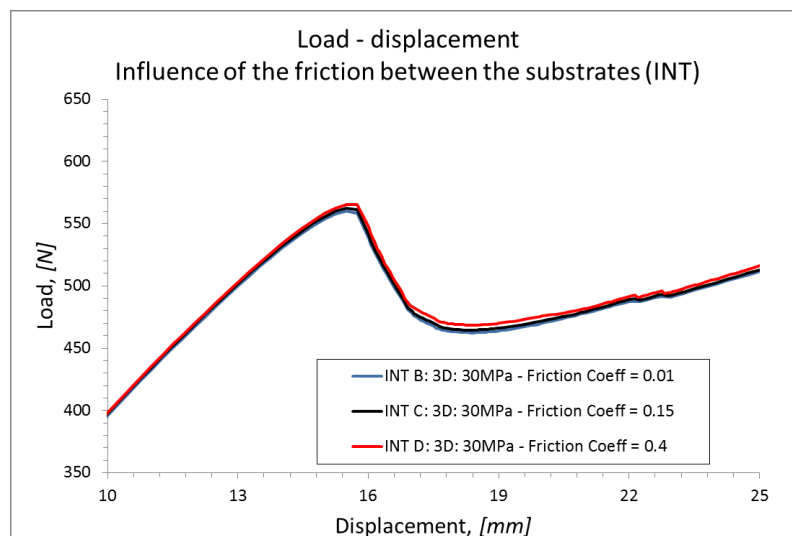

Figure 7 influence of the friction between the substrates (INT) on the numerical load-displacement curves of the ENF simulation

External friction between the substrates and the rods

Here, the effect of the friction between the rods and the substrates is investigated. Since in reality these rods are supposed to produce very little friction, the values for the friction coefficient were varied between 0.01 for model EXT A, 0.33 for model EXT B and 0.4 for model EXT C. The strength τ^0 at failure initiation used for this investigation equals 30 MPa. All the results of the output were written out at each time increment of the simulation.

Although the shape of the load-displacement curves of the results (Figure 8) remains similar, a big shift in loads can be observed. A difference between the minimum load for model EXT A (corresponding to almost no friction) and model EXT C reaches up to 8% which is not negligible. This means that in the reports of an experimental ENF analysis should be mentioned what this friction coefficient was.
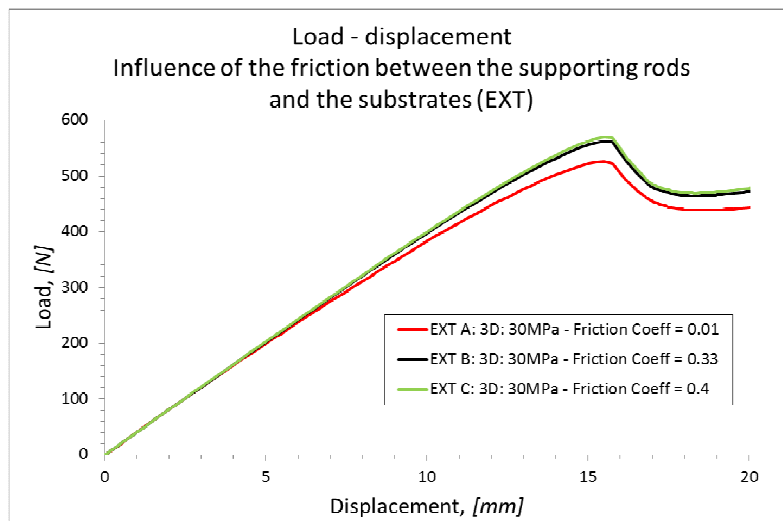

Figure 8 Influence of the friction between the substrates and the rods (EXT) on the numerical load-displacement curves of the ENF simulation

Combination of friction and strength

When combining the influences due to the external friction and the strength in one graph (Figure 9) it is obvious that these effects impact a lot the simulated results. A difference in maximum force between the minimum value obtained with model COM C and the maximum value obtained with model COM D represents an increase of approximately 20%.
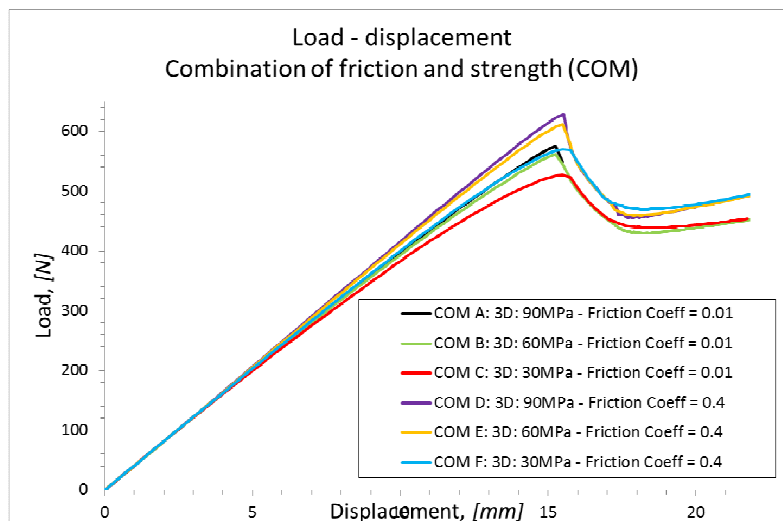

Figure 9 Load-displacement curves of ENF numerical simulations with combinations of influences due to friction and strength

If the lessons from these studies are applied to the simulation of an ENF test one obtains a good correlation between the experimental results (CET 7 and CET 8) as defined in section 2 and the numerical load-displacement curves (Figure 10). The analytical curves have been constructed with the maximum and minimum critical strain energy release rates G_{IIc} defined experimentally . The difference between the experimental and analytical results is due to the friction between the rods and the substrates and the failure strength τ^0 in the traction-separation law. This proves the added value of such numerical simulations.
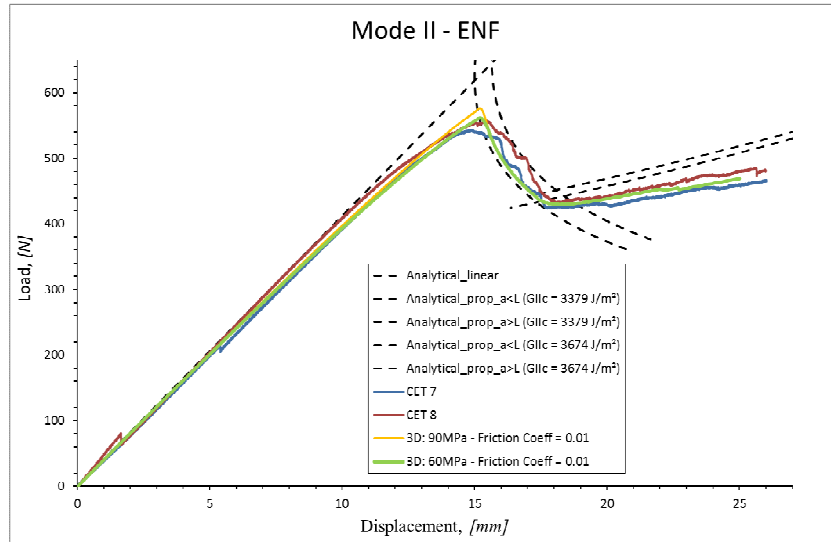

Figure 10 Load-displacement curves of the ENF numerical and experimental test results

4 CONCLUSIONS

When performing simulations using the cohesive model approach for delamination growth, attention must be paid to using the correct combination of numerical parameters such as stiffness, strength and the traction-separation law, numerical stabilization, output frequency, mesh size. Once convergence was achieved, the influence of different experimental parameters, such as the difference in thickness of the substrates of the specimen, the positioning of the supporting and loading rods, the influence of friction, both between the substrates and between the specimen and the supports was investigated. It could be concluded that a small change in thickness of one of the two substrates composing the ENF specimen did not lead other results. A same conclusion can be drawn concerning the friction between the two substrates. Small rotations of either the supporting rods or the loading rod did not influence the force-displacement curves. However, the friction between the specimen and the supporting rods leads to different results between the crack propagation parts of the load-displacement curves and the translation of the supporting or loading rolls influences the entire load-displacement curves.

A general conclusion when dealing with numerical and experimental tests of delaminations in general is that when one wants to achieve a correlation between the experimental and numerical curves, it would be better to give a range in which the numerically obtained curves would be using different parameters, than giving a result correlating with one curve because of the impact of the different numerical parameters. It is advised that for all numerical simulations all details needed for the numerical simulations would be given in the manuscripts.

REFERENCES

[1] J D Barrett and R O Foschi, "Mode II stress-intensity factors for cracked wood beams," *Engineering fracture mechanics*, vol. 9, pp. 371-378, 1977.

[2] P S Vanderkley, *Mode I - Mode II delamination fracture toughness of a unidirectional graphite/epoxy composite, Master thesis*. Texas: Texas A&M University, 1981.

[3] L A Carlsson and J W Gillespie, "Mode II interlaminar fracture of composites," *Application of fracture mechanics to composite materials*, 1989.

[4] D Davies et al., "Comparison of test configurations for the determination of GIIc: results from an international round robin," *Plastics, Rubber and Composites*, vol. 28, no. 9, pp. 432-437, September 1999.

[5] A Turon, P P Camanho, J Costa, and C G Dávila, "A damage model for the simulation of delamination in advanced composites under variable-mode loading," *Mechanics of Materials*, vol. 38, pp. 1072-1089, 2006.

[6] Jacques S., De Baere I. and Van Paepegem W. Analysis of the numerical and geometrical parameters influencing the simulation of mode I and mode II delamination growth in unidirectional and textile composites. *Applied Composite Materials*, (doi: 10.1007/s10443-014-9429-9

[7] Ives De Baere, Stefan Jacques, Wim Van Paepegem, and Joris Degrieck, "Study of the Mode I and Mode II interlaminar behaviour of a carbon fabric reinforced thermoplastic," *Polymer Testing*, vol. 31, no. 2, pp. 322-332, April 2012.

[8] P P Camanho, A Turon, C Sarrado, G Guillamet, and D Trias, "Simulation of delamination in polymer composites: best practices at different levels of analysis.," in *Technical interchange meeting ESA/ESTEC*, Noordwijk, 2011.

[9] J Quintelier et al., "Wear behavior of carbon fiber reinforced Poly Phenylene Sulfide," *Polymer Composites*, vol. 27, no. 1, pp. 92-98, 2006.

[10] BearingWorks. Bearing Works inc. [Online]. http://www.bearingworks.com/content_files/pdf/retainers/PPS%20datasheet.pdf